Oxidative Modification of Proteasome: Identification of an Oxidation-Sensitive Subunit in 26 S Proteasome†

Takeshi Ishii,‡ Toyo Sakurai,‡ Hiroko Usami,‡ and Koji Uchida*,‡,§

Graduate School of Bioagricultural Sciences, and Institute for Advanced Research, Nagoya University, Nagoya 464-8601, Japan

Received July 11, 2005; Revised Manuscript Received August 19, 2005

ABSTRACT: Reactive oxygen species (ROS) have the potential to damage cellular components, such as protein, resulting in loss of function and structural alteration of proteins. The oxidative process affects a variety of side amino acid groups, some of which are converted to carbonyl compounds. We have previously shown that a prostaglandin D_2 metabolite, 15-deoxy-$\Delta^{12,14}$-prostaglandin J_2 (15d-PGJ_2), is the potent inducer of intracellular oxidative stress on human neuroblastoma SH-SY5Y cells [Kondo, M., Oya-Ito, T., Kumagai, T., Osawa, T., and Uchida, K. (2001) Cyclopentenone prostaglandins as potential inducers of intracellular oxidative stress, *J. Biol. Chem. 276*, 12076−12083]. In the present study, to elucidate the molecular mechanism underlying the oxidative stress-mediated cell degeneration, we analyzed the protein carbonylation on SH-SY5Y cells when these cells were submitted to an endogenous inducer of ROS production. Upon exposure of SH-SY5Y cells to this endogenous electrophile, we observed significant accumulation of protein carbonyls within the cells. Proteomic analysis of oxidation-sensitive proteins showed that the major intracellular target of protein carbonylation was one of the regulatory subunits in 26 S proteasome, S6 ATPase. Accompanied by a dramatic increase in protein carbonyls within S6 ATPase, the electrophile-induced oxidative stress exerted a significant decrease in the S6 ATPase activities and a decreased ability of the 26 S proteasome to degrade substrates. Moreover, in vitro oxidation of 26 S proteasome with a metal-catalyzed oxidation system also confirmed that S6 ATPase represents the most oxidation-sensitive subunit in the proteasome. These and the observation that down-regulation of S6 ATPase by RNA interference resulted in the enhanced accumulation of ubiquitinated proteins suggest that S6 ATPase is a molecular target of ROS under conditions of electrophile-induced oxidative stress and that oxidative modification of this regulatory subunit of proteasome may be functionally associated with the altered recognition and degradation of proteasomal substrates in the cells.

Several lines of evidence indicate that oxidative stress may play an important role in various pathological states including cancer, neurodegeneration, atherosclerosis, diabetes, and rheumatoid arthritis, as well as in drug-associated toxicity, postischemic reoxygenation injury, and aging (*1*). Oxidative stress is also seen as a major upstream component in the signaling cascade involved in many of the cellular functions, such as cell proliferation, inflammatory responses, stimulating adhesion molecule, and chemoattractant production (*1*). It has been suggested that some level of oxidative stress may be required in response to cytotoxic agents and converted into the redox regulatory system as a downstream signaling pathway (*2*). However, excess oxidative stress may be toxic, exerting cytostatic effects, causing membrane damage, and activating pathways of cell death (apoptosis and/or necrosis). Reactive oxygen species (ROS)[1] resulting from episodes of oxidative stress are responsible for these effects due to their ability to damage cellular components, such as protein. The oxidative modification of proteins by ROS has been implicated in the etiology or progression of a wide range of disorders and diseases.

The oxidative damage to proteins is reflected by increase in levels of protein carbonyls (*3*). In view of the fact that protein carbonyls are formed by many different processes, a number of simple, highly sensitive, specific methods for the assay of protein carbonyls have been developed (*4*−*6*). The utilization of these methods has allowed the carbonyl content of proteins to become a widely used marker of ROS-mediated damage during oxidative stress, aging, and in age-related diseases. The increased levels of protein carbonyls have been reported to be associated with Alzheimer's disease (*7*), progeria and Werner's syndrome (*6*), amyotrophic lateral sclerosis (*8*), and respiratory distress syndrome (*9*), among others. Although the experimental evidence is so far mostly correlative, it lends strong support to the hypothesis that the protein carbonyl content of tissues reflects the fraction of oxidatively damaged protein with impaired function and

† This work was supported by a research grant from the Ministry of Education, Culture, Sports, Science, and Technology and by the COE Program in the 21st Century in Japan.

* To whom correspondence should be addressed: Koji Uchida, Laboratory of Food and Biodynamics, Graduate School of Bioagricultural Sciences, Nagoya University, Nagoya 464-8601, Japan. Fax: 81-52-789-5741. E-mail: uchidak@agr.nagoya-u.ac.jp.

‡ Graduate School of Bioagricultural Sciences, Nagoya University.

§ Institute for Advanced Research, Nagoya University.

[1] Abbreviations: ROS, reactive oxygen species; 15d-PGJ_2, 15-deoxy-$\Delta^{12,14}$-prostaglandin J_2; biotin-LC-hydrazide, EZ-Link biotin-LC-hydrazide; DTT, dithiothreitol; ELISA, enzyme-linked immunosorbent assay; HRP, horseradish peroxidase; PBS, phosphate-buffered saline; MALDI-TOF, matrix-assisted laser desorption ionization-time-of-flight; ODC, ornithine decarboxylase; RNAi, RNA interference; siRNA, short interfering RNA.

10.1021/bi051336u CCC: $30.25
Published on Web 09/30/2005

might therefore be at the root of disease- and aging-related functional losses (*10*).

In our previous study, to identify the endogenous inducer of intracellular oxidative stress, we examined the oxidized fatty acid metabolites for their ability to induce intracellular ROS production in SH-SY5Y human neuroblastoma cells in vitro and found that 15-deoxy-$\Delta^{12,14}$-prostaglandin J_2 (15d-PGJ_2) represents the most potent inducer (*11*). In addition, we demonstrated for the first time that 15d-PGJ_2 was accumulated in the spinal cord of sporadic amyotrophic lateral sclerosis patients, mainly occurring in the motor neurons of the anterior horn (*12*). These findings raised the possibility that cyclooxygenase-2 up-regulation, through its pivotal role in inflammation, followed by the enhanced intracellular production of 15d-PGJ_2, might be ubiquitously involved in neurodegenerative processes. In the present study, to elucidate the molecular mechanism underlying the oxidative stress-mediated cell degeneration, we analyzed protein carbonyls generated in human neuroblastoma SH-SY5Y cells exposed to 15d-PGJ_2 and identified a 19 S regulatory cap as a molecular target of protein oxidation under conditions of electrophile-induced oxidative stress.

EXPERIMENTAL PROCEDURES

Materials. 15d-PGJ_2 was obtained from the Cayman Chemical Co. (Ann Arbor, MI). H_2O_2 (31% aqueous solution) was obtained from Mitsubishi Gas Co. The anti-ubiquitin polyclonal antibody was obtained from Biomega Co. (Foster City, CA). Horseradish peroxidase (HRP)-conjugated NeutrAvidin, HRP-linked anti-rabbit IgG and enhanced chemiluminescence (ECL) Western blotting detection reagents were obtained from Amersham Biosciences. Biotin-LC-hydrazide was obtained from Pierce. Anti-FLAG antibody was obtained from Sigma. SYPRO Ruby protein gel stain was from Molecular Probes, Inc. Sequence grade modified trypsin was obtained from Promega. Dithiothreitol (DTT) and iodoacetoamide were obtained from Wako Pure Chemical Industries, Ltd. pcDNA-FLAG-ubiquitin was kindly provided by Dr. Hideki Shibata (Nagoya University).

Cell Culture. SH-SY5Y cells were grown in Cosmedium-001 (Cosmo-Bio, Tokyo) containing 5% Nakashibetsu precolostrum new-born calf serum, 100 μg/mL penicillin, and 100 units/mL streptomycin in a 5% CO_2-containing atmosphere. The cells were seeded in plates coated with polylysine and cultured at 37 °C.

Metal-Catalyzed Oxidation of Purified 26 S Proteasome. The purified 26 S proteasome (~95% purity; specific activity, 25 units/mg) from human erythrocytes was obtained from the Affiniti Research Products, Ltd. (Exeter, U.K.). The 26 S proteasome (10 μg) was incubated with H_2O_2 (0−1 mM) and Cu^{2+} (10−1000 μM) in PBS for 30 min at 25 °C.

Sample Preparation and Biotin Derivatization of Protein Carbonyls. Cells were incubated with 20 μM 15d-PGJ_2 in a control medium for 0 ~ 6 h. The medium was removed and then washed twice with PBS, lysed with a sonicator in lysis buffer (50 mM sodium acetate buffer (pH 4.5) and protease inhibitors), and centrifuged at 10 000 rpm for 5 min at 4 °C; the supernatant was assayed for protein content. Biotin-LC-hydrazide was employed to detect protein-bound carbonyls (*13*). The biotin-LC-hydrazide solution (18.6 mg/mL in DMSO) was added to the cell lysate to a final concentration of 1 mM, and the cell lysate was shaken for 1 h at room temperature in order for protein carbonyls to be biotinylated.

ELISA Analysis of Protein Carbonyls. A 100-μL aliquot of the protein solution was added to each well of a 96-well microtiter plate and incubated for 20 h at 4 °C. The solution was then removed, followed by washing with PBS containing 0.05% Tween 20 (PBS/Tween); 100 μL of the 1 mM biotin-LC-hydrazide in a solution containing 50 mM sodium acetate buffer (pH 4.5) was added to the wells. After incubation for 1 h at 37 °C, followed by washing with the PBS/Tween, each well was filled with 200 μL of Block Ace solution (40 mg/mL) for 1 h at 37 °C. The peroxidase-conjugated NeutrAvidin solution was added and the mixture incubated for 1 h at 37 °C. After washing, 100 μL of 50 mM citrate buffer (pH 5.5) containing *o*-phenylenediamine (0.4 mg/mL) and 0.003% H_2O_2 was added and the mixture incubated for several minutes at room temperature. The reaction was terminated by adding 50 μL of 2 M sulfuric acid, and the absorbance at 490 nm was read on a micro-ELISA plate reader.

Dot Blot and Western Blot Analyses. For detection of ubiquitinated proteins, whole cell lysates from SH-SY5Y cells were treated with SDS sample buffer with reducing agent for 5 min at 100 °C. For detection of the protein carbonyls, the cell lysates were labeled with biotin-LC-hydrazide prior to the treatment with the sample buffer. The samples were then transblotted or separated by 10 or 12.5% sodium dodecyl sulfate−polyacrylamide gel electrophoresis (SDS−PAGE). The gel was transblotted onto a nitrocellulose or PVDF membrane. The membranes were incubated with 5% skim milk for blocking, washed, and incubated with the HRP−NeutrAvidin. This procedure was followed by the addition of ECL reagents. The spots were visualized by Cool Saver AE-6955 (ATTO, Tokyo, Japan).

Protein Separation by One-Dimensional and Two-Dimensional Electrophoresis. For the detection of protein carbonyls by one-dimensional electrophoresis, the total cell lysates treated with reducing agent were heated at 100 °C for 5 min and resolved by 12.5% SDS−PAGE, and proteins were transferred to the PVDF membrane for Western blot analysis.

For the identification of carbonylated proteins by two-dimensional electrophoresis, samples containing 300 μg of total cell lysate (supplemented with 1% immobilized pH gradient (IPG) buffer, pH 3−10) were used to rehydrate IPG strips, pH 3−10 (Amersham Biosciences, Inc.). First dimension electrophoresis was performed using the following program: 1 h at 500 V, 1 h at 1000 V, 6 h at 8,000 V. Prior to second dimension electrophoresis, IPG strips were equilibrated for 20 min in 50 mM Tris-HCl (pH 6.8), 6M urea, 30% glycerol, 2% SDS, and 0.01% bromphenol blue with reducing and alkylating agent. The second dimension was performed on a gradient gel (4−12%) at a constant 25 mA per gel. Separated proteins were then fixed in the gel using 40% ethanol and 10% formic acid, stained with SYPRO Ruby protein gel stain, and scanned using the Typhoon 9400 (Amersham Biosciences, Inc.). Western blot analyses were previously described. The protein spots were visualized by Image Quant (Amersham Biosciences, Inc.).

Identification of Carbonylated Proteins. Gel pieces were washed in water containing 10 mM ammonium bicarbonate buffer (pH 8.0) and 50% methanol for 1 h, dehydrated in acetonitrile, and dried in a SpeedVac for 30 min. Samples

were proteolyzed with 100−500 ng of sequence grade modified trypsin in 50 mM Tris-HCl buffer (pH 8.8) overnight at 37 °C. The supernatant was collected, and peptides were further extracted with water containing 0.1% TFA, 50% acetonitrile containing 0.1% TFA, and acetonitrile. Peptide extracts were vacuum-dried and resuspended in water containing 0.1% TFA.

Peptide mass fingerprints were generated with an AutoFLEX matrix-assisted laser desorption ionization-time-of-flight (MALDI-TOF) mass spectrometer (Bruker Daltonics Japan, Ltd., Tokyo, Japan). A few microliters of the sample were mixed with an equal volume of a saturated solution of *a*-ciano-4-hydroxycinnamic acid (Bruker Daltonics) in 50% acetonitrile containing 0.1% TFA; 1 μL of the mixture was deposited on the MALDI-TOF mass spectrometry target. Proteins were identified with the MASCOT (Matrix Science, London, U.K.) searching algorithms using the nonredundant database. Probability-based MOWSE scores were estimated by comparison of search results against estimated random match population and were reported as $\sim 10*\mathrm{LOG}_{10}(p)$, where p is the absolute probability. Scores greater than 63 were considered significant, meaning that for scores higher than 63 the probability that the match is a random event is lower than 0.05. All protein identifications were in the expected size and PI range based on position in the gel.

Pull-Down and Immunoprecipitation Assays. SH-SY5Y cells incubated with and without 20 μM 15d-PGJ_2 in a control medium for 6 h were washed with PBS, harvested, and lysed in 10 mM Tris-HCl, (pH 7.4), 5 mM EDTA, 150 mM NaCl, 1% NP-40, and protease inhibitors. Cell lysates containing 1 mg of protein were incubated batch-wise with 50 μL of StreptAvidin-Plus beads overnight at 4 °C with constant shaking. The beads were rinsed five times with lysis buffer by centrifugation at 3000 rpm for 5 min. The proteins were eluted by boiling the beads in Laemmli sample buffer for 5 min and analyzed by SDS−PAGE followed by immunodetection with anti-S6 ATPase polyclonal antibody. In addition, the cell lysates were incubated with 3 μg of anti-S6 ATPase antibody overnight at 4 °C. The mixture was then treated with 20 μL of Protein G-Sepharose (Amersham Pharmacia Biotech) and incubated for 1 h at 4 °C. The mixture was then centrifuged (3000 rpm, 5 min), rinsed five times with lysis buffer, and then boiled with the Laemmli sample buffer, and the biotinylated proteins were then subjected to immunoblot and detection with HRP-conjugated NeutrAvidin and ECL.

Ubiquitin-Dependent Proteolysis. We measured the ability of cell lysates from either control or 15d-PGJ_2-treated cells to degrade ubiquitinated proteins. FLAG-tagged ubiquitin transfected SH-SY5Y cells were treated with MG132 for 6 h, and the cells were lysed with a sonicator in lysis buffer (10 mM Tris-HCl (pH 7.4), 5 mM EDTA, 150 mM NaCl, 1% NP-40, and protease inhibitors) and then centrifuged at 10 000 rpm for 5 min at 4 °C. The resulting lysates containing FLAG-ubiquitinated proteins were coated overnight at 4 °C on the wells of the 96-well microtiter plate. After washing with PBS containing 0.05% Tween 20 (PBS/Tween), the coated FLAG-ubiquitinated proteins were incubated with cell lysates either from untreated control cells or 15d-PGJ_2-treated cells in 50 mM Tris-HCl (pH 7.5) containing 5 mM $MgCl_2$, 2 mM ATP, 1 mM DTT, and ATP regenerating system. After incubation for 1 h at 37 °C, the solution was then removed, and the plate was washed with Tris-buffered saline (TBS) containing 10% Tween 20 (TBS/Tween). Each well was incubated with 200 μL of Block Ace solution (40 mg/mL) in TBS/Tween for 30 min at 37 °C in a moist chamber to block the unsaturated plastic surface. The plate was then washed once with TBS/Tween. A 100-μL aliquot of anti-FLAG-antibody solution was added to each well and incubated for 1 h at 37 °C. After discarding the supernatants and washing three times with TBS/Tween, 100 μL of a 5×10^4 dilution of goat anti-mouse IgG conjugated to horseradish peroxidase in TBS/Tween was added. After incubation for 1 h at 37 °C, the supernatant was discarded, and the plates were washed three times with TBS/Tween. Enzyme-linked antibody bound to the well was revealed by adding 100 μL/well of 1,2-phenylenediamine in 0.1 M citrate/phosphate buffer (pH 5.0) containing 0.003% hydrogen peroxide. The reaction was terminated by the addition of 50 μL of 2 M sulfuric acid, and absorbance at 492 nm was read on a micro-ELISA plate reader.

ATPase Assay. ATPase activities were assayed on anti-S6 ATPase immunoprecipitates that had been collected on 20 μL of packed protein G-Sepharose beads. Immunoprecipitates were washed four times with 1 mL of 50 mM Tris-HCl, pH 7.4, 0.5 M NaCl, 5% sucrose (w/v), 1 mM EDTA, and 1% NP-40. Immunoprecipitates subsequently were washed twice more with 1 mL of 20 mM Tris-HCl, pH 7.4. Washed beads were then resuspended in 30 μL of 5 μM ATP in a solution containing 20 mM Tris-HCl, pH 7.4, 100 μM $MgCl_2$, and 2 mM dithiothreitol (DTT). Reactions proceeded for 15 min at 30 °C prior to quantification of released phosphate.

RNA Interference Using siRNA. The following siRNA was generated by Invitrogen: human S6 ATPase (sequence no. 1118-1142, 5′-GCCAGAUAAGAUUUCAGGAGCUGAU-3′). For a control, we used Stealth RNAi Negative Control Duplexes (Invitrogen). SH-SY5Y cells were seeded at 80% density the day before transfection. Cells were transfected with Lipofectamine2000 transfection reagent; 2.5 μL of siRNA stock (20 μM) and 5 μL of Lipofectamine2000 were each diluted with 250 μL of Opti-MEM (Invitrogen). After 5 min at room temperature, they were combined and incubated for 20 min. The reaction mixtures were overlaid on the cell culture for 6 or 12 h. The medium was then changed to a fresh medium containing 5% FBS.

RESULTS

Detection of Protein Carbonyls in SH-SY5Y Cells Exposed to an Endogenous Electrophile. To analyze protein carbonyls generated in the cells, we utilized biotin-LC-hydrazide (Figure 1A) as the molecular probe. The presence of a biotin tag on proteins, which form a hydrazone bond, allows a range of investigative procedures to be carried out which exploit the high affinity of biotin for avidin derivatives. After exposure to 15d-PGJ_2, whole cell lysates were labeled with this carbonyl reagent, and the biotin-labeled protein carbonyls were analyzed by dot blot and Western blot probed with streptavidin−HRP. Consistent with our previous findings that 15d-PGJ_2 stimulates intracellular oxidative stress monitored by lipid peroxidation (*12*) and protein *S*-thiolation (*14*), 15d-PGJ_2 significantly enhanced the productions of protein carbonyls in SH-SY5Y cells (Figure 1, panels B and C). On

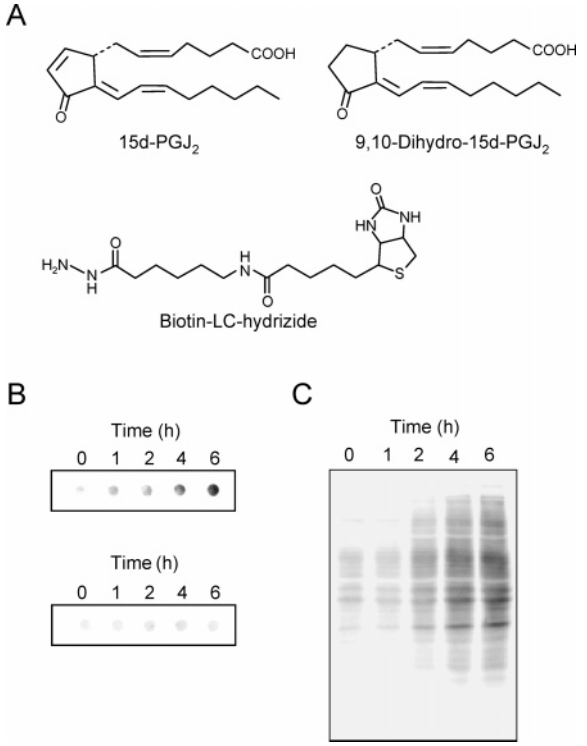

FIGURE 1: Detection of protein carbonyls in SH-SY5Y cells exposed to an endogenous electrophile. (A) Chemical structures of 15d-PGJ_2, 9,10-dihydro-15d-PGJ_2, and biotinylated hydrazine (biotin-LC-hydrazide). (B) Dot blot analysis of biotin-LC-hydrazide-protein adducts. Upper panel, detection of protein carbonyls in the 15d-PGJ_2-treated cells; lower panel, detection of protein carbonyls in the 9,10-dihydro-15d-PGJ_2-treated cells. (C) Western blot analysis of biotin-LC-hydrazide-protein adducts. In panels B and C, cells were incubated with 10 μM 15d-PGJ_2 for 1 h and then treated with 1 mM biotin-LC-hydrazide for 1 h. Total cell lysate was heated at 95 °C for 5 min and resolved by SDS−PAGE followed by dot blot and Western blot analyses.

the other hand, 9,10-hihydro-15d-PGJ_2, an analogue of 15d-PGJ_2, had no significant effects on the ROS production (Figure 1B), suggesting that these pro-oxidant activities could be attributed to the electrophilic center of 15d-PGJ_2.

Identification of Carbonylated Proteins. To identify the carbonylated protein, the biotin-LC-hydrazide-labeled proteins were separated by two-dimensional gel electrophoresis and analyzed by Western blot probed with streptavidin−HRP. As shown in Figure 2 (panels A and B), two proteins (spots no. 1 and no. 2) were clearly visible for the 15d-PGJ_2-treated cell preparations. These spots were further subjected to proteomic identification: they were excised from two-dimensional gels, subjected to trypsin digestion, and analyzed by MALDI-TOF MS. Peptide mass fingerprint analysis of the 48-kDa protein (spot no. 1) revealed selective oxidation of a 19 S regulatory subunit, S6 ATPase [using MASCOT, the provability-based MOWSE score was 103 for 19 S regulatory subunit 6 (S6 ATPase) ($p < 0.05$), with 8 peptide matches (error ±0.05%), which represents 21% sequence coverage] (Figure 2C and Table 1). The formation of protein carbonyls into endogenous S6 ATPase was further confirmed by pull-down with NeutrAvidin beads followed by Western blot with an anti-S6 ATPase antibody (Figure 2D, left panel). Alternatively, cell lysates were subjected to immunoprecipitation with an anti-S6 antibody, and the presence of protein-bound carbonyls was detected by Western blot analysis with HRP-conjugated NeutrAvidin (Figure 2D, right panel). These

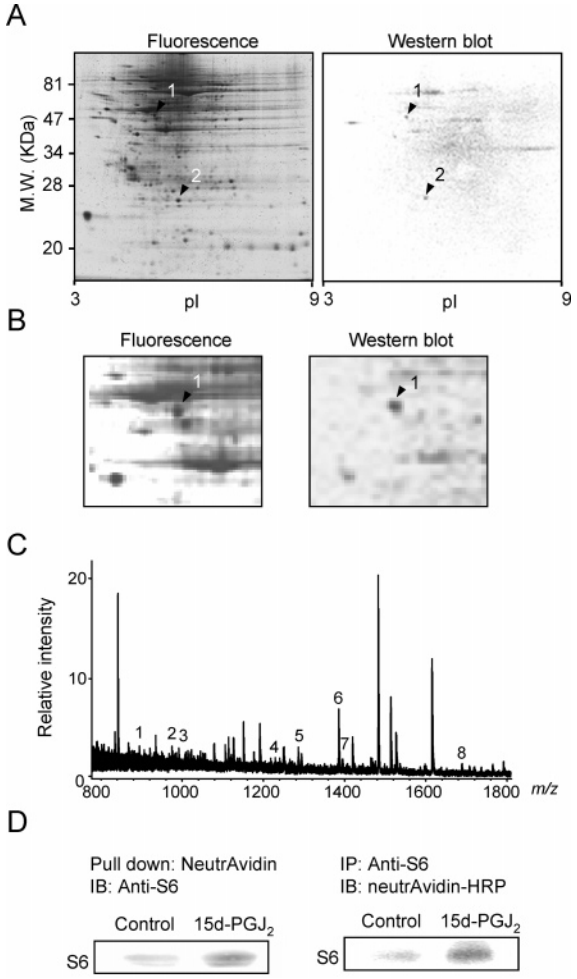

FIGURE 2: Identification of carbonylated proteins in SH-SY5Y cells exposed to an endogenous electrophile. SH-SY5Y cells were incubated with 20 μM 15d-PGJ_2 for 6 h and then treated with 1 mM biotin-LC-hydrazide for 1 h. The proteins were separated by isoelectrofocusing (pH range 3−10) and then by SDS−PAGE. (A) Left panel, SYPRO Ruby fluorescence staining; right panel, Western blot. The arrowheads denote spots (no. 1 and no. 2) excised for subsequent identification by MALDI-TOF analysis, as described under Experimental Procedures. (B) Enlarged view around spot no. 1. Left panel, SYPRO Ruby fluorescence staining; right panel, Western blot. (C) Identification of S6 ATPase as the target of protein carbonylation. MALDI-TOF MS spectrum corresponding to S6 ATPase tryptic digest. The *m*/*z* values obtained from tryptic peptides were used to identify the protein by searching in database. The elution positions of the identified tryptic peptides are indicated in the total ion current and summarized in Table 1. (D) Protein carbonylation of endogenous S6 ATPase in SH-SY5Y cells exposed to 15d-PGJ_2. SH-SY5Y cells were incubated with 20 μM 15d-PGJ_2 for 6 h and then treated with 1 mM biotin-LC-hydrazide for 1 h. Cell lysates were incubated with Immobilized NeutrAvidin or with anti-S6 ATPase-sepharose, as indicated. The presence of oxidized S6 ATPase was detected by immunoblot analysis (left panel), and the incorporation of biotin-LC-hydrazide into S6 ATPase immunoprecipitates was detected with HRP−NeutrAvidin and ECL (right panel).

and the observation that H_2O_2 treatment of the cells also gave rise to the oxidative modification of S6 ATPase (Figure 3) suggest that this proteasome subunit may represent a general target of intracellular ROS. On the other hand, the 23-kDa protein (spot no. 2) was identified to be glutathione-*S*-transferase P1 by peptide mass fingerprint analysis (Supporting Information, Figure S1), while this identification has

Table 1: Peptides Identified by MALDI-TOF MS from a Carbonylated Protein (spot no. 1)[a]

position	calculated mass	observed mass	error (Da)	peptide sequence	peak no.
71−80	1229.61	1229.66	0.05	EFLHAQEEVK	4
122−134	1419.82	1419.84	0.02	ELLKPNASVALHK	7
179−192	1688.88	1688.93	0.05	EAVELPLTHFELYK	8
193−200	895.49	895.47	−0.02	QIGIDPPR	1
218−229	1294.69	1294.71	0.02	AVAHHTTAAFIR	5
230−238	992.53	992.53	0	VVGSEFVQK	2
314−326	1394.77	1394.79	0.02	ADTLDPALLRPGR	6
343−351	1009.59	1009.58	−0.01	LIFSTITSK	3

[a] The *m*/*z* values obtained from tryptic peptides were used to identify the protein by searching in database.

not been confirmed by the pull-down/immunoprecipitation technique.

Impairment of Proteasome Functions. The ubiquitin/proteasome system degrades most proteins in the cytosol and nucleus of eukaryotic cells (*15*−*17*). It is important for the regulation of cellular processes, including cell cycle progression, transcription, and antigen processing. Consequently, aberrations of this pathway have been implicated in the pathogenesis of many diseases. Proteins requiring degradation are covalently conjugated with multiple ubiquitin moieties, making them targets for the large multicatalytic 26 S proteasome (*15*−*17*). The 26 S proteasome comprises two subcomplexes: a barrel-shaped 20 S core complex, which exhibits catalytic activity; and two regulatory 19 S cap complexes, each bound to opposite ends of the 20 S core complex (*15*, *17*). The regulatory 19 S cap complex of the 26 S proteasome confers the specificity toward ubiquitinated substrates and an ATP dependence on proteolysis (*18*, *19*). To assess if oxidative modification of S6 ATPase elicited by 15d-PGJ_2 in SH-SY5Y cells could result in the impairment of its enzyme function, changes in cellular S6 ATPase activity were examined. To this end, SH-SY5Y cells were treated with 15d-PGJ_2, and ATPase activities were assayed on anti-S6 ATPase immunoprecipitates. Simultaneously, the levels of S6 ATPase-bound carbonyls were examined by immunoblot analysis with HRP−NeutrAvidin following the biotin-LC-hydrazide labeling. As shown in Figure 4A, accompanied by a dramatic increase in protein carbonyls within the S6 ATPase subunit (upper panel), 15d-PGJ_2 treatment exerted a significant decrease in the ATPase activities (lower panel).

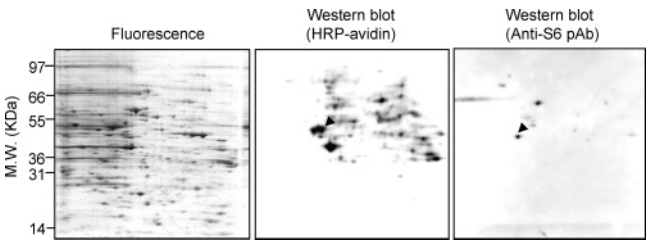

FIGURE 3: Identification of carbonylated proteins in SH-SY5Y cells exposed to H_2O_2. SH-SY5Y cells were incubated with 1 mM H_2O_2 for 30 min and then treated with 1 mM biotin-LC-hydrazide for 1 h. The proteins were separated by isoelectrofocusing (pH range 3−10) and then by SDS−PAGE. Left panel, SYPRO Ruby fluorescence staining; middle panel, Western blot analysis with HRP−NeutrAvidin; right panel, Western blot analysis with anti-S6 ATPase antibody. The arrowheads denote identical spots in the middle and right panels.

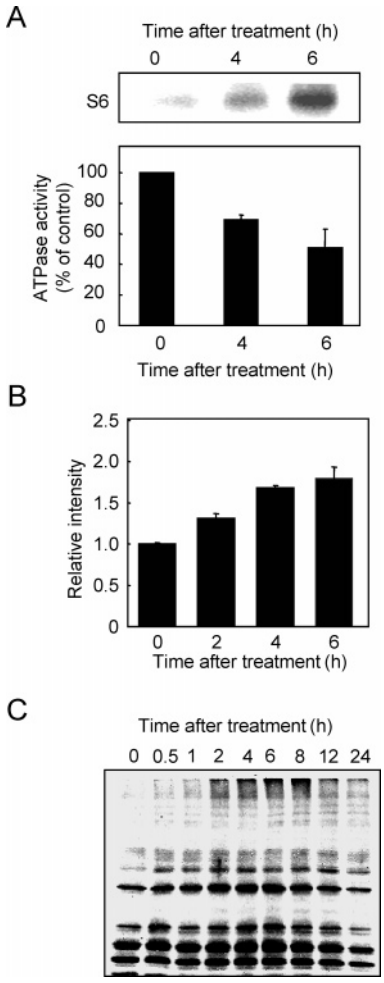

FIGURE 4: Impairment of S6 ATPase in SH-SY5Y cells exposed to an endogenous electrophile. (A) Formation of protein carbonyls on S6 ATPase and concomitant loss of S6 ATPase activity in SH-SY5Y cells treated with 15d-PGJ_2. The levels of S6 ATPase-bound carbonyls were examined by immunoblot analysis with HRP−NeutrAvidin following the biotin-LC-hydrazide labeling (upper panel). Simultaneously, the ATPase activities were assayed on anti-S6 ATPase immunoprecipitates (lower panel). (B) Effect of 15d-PGJ_2 on proteasome activity evaluated by ELISA with anti-FLAG antibody as described under Experimental Procedures. The relative intensity at 0 time represents the proteasome activity in the cells without treatment with 15d-PGJ_2. (C) Effect of 15d-PGJ_2 on accumulation of ubiquitinated proteins in SH-SY5Y cells. The ubiquitinated proteins were detected by immunoblot analysis using an anti-ubiquitin polyclonal antibody.

The ROS-mediated oxidation of the 19 S regulatory subunit, observed during the electrophile treatment, was expected to have an effect on the integrity and function of the 26 S proteasome as well as protein turnover in the dying cell. To test this hypothesis, we measured the ability of cell lysates from either control or 15d-PGJ_2-treated cells to degrade ubiquitinated proteins. FLAG-tagged ubiquitin was expressed stably in SH-SY5Y cells, and the ability of cell lysates from either control or 15d-PGJ_2-treated cells to degrade FLAG-ubiquitinated proteins was verified by ELISA with anti-FLAG antibody. As shown in Figure 4B, the ubiquitinated proteins were degraded much more effectively by the lysates from control than those from 15d-PGJ_2-treated cells. In addition, 15d-PGJ_2 significantly enhanced the accumulation of ubiquitinated proteins (Figure 4C). The level of ubiquitinated proteins increased during 8 h of incubation and then decreased thereafter. These data suggest that

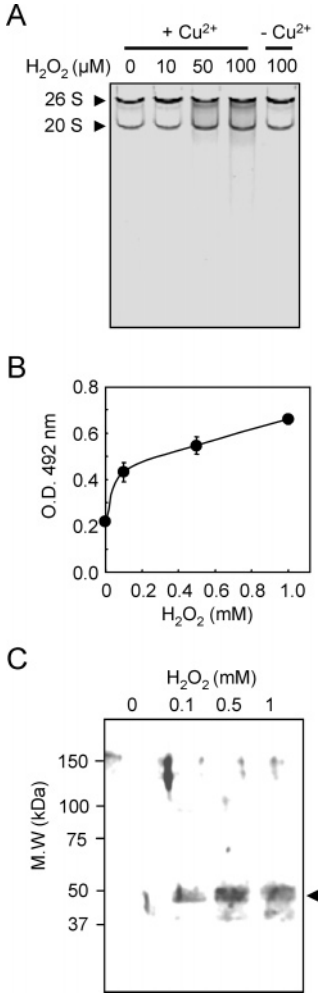

FIGURE 5: Metal-catalyzed oxidation of purified 26 S proteasome. (A) Polyacrylamide gel electrophoresis of 26 S proteasome treated with H_2O_2 in the presence or absence of Cu^{2+}. The 26 S proteasome (10 μg/mL) was incubated with 0−1 mM H_2O_2 in the absence and the presence of 10 μM Cu^{2+}. (B) ELISA analysis of protein carbonyls. (C) Western blot analysis of protein carbonyls. In panels B and C, the 26 S proteasome (10 μg/mL) was incubated with 0−1 mM H_2O_2 in the absence and the presence of 100 μM Cu^{2+}. Aliquots were sampled at the indicated times, labeled with biotin-LC-hydrazide, and analyzed for protein carbonyls by ELISA and Western blot.

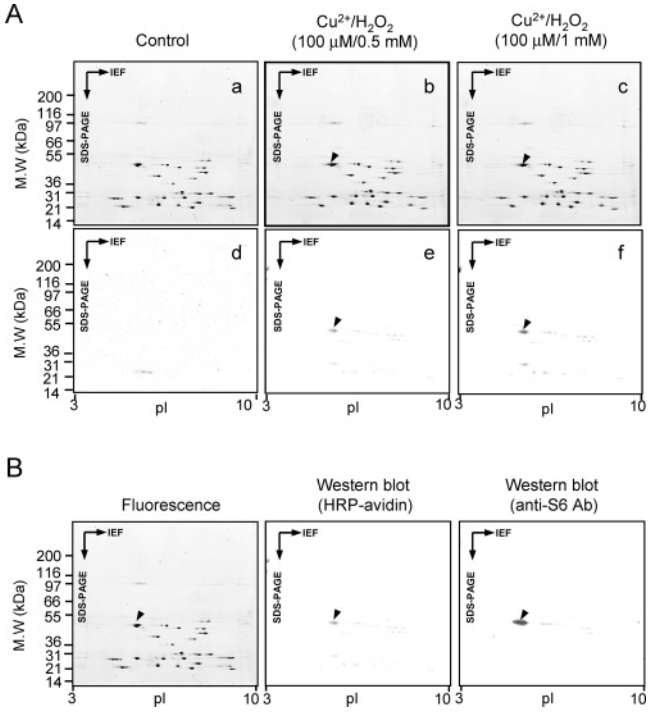

FIGURE 6: Identification of the ROS-sensitive subunit in purified 26S proteasome. (A) Detection of a specific target of ROS in 26 S proteasome. To identify the carbonylated protein, the biotin-LC-hydrazide-labeled proteins were separated on two-dimensional gel electrophoresis and analyzed by Western blot probed with streptavidin−HRP. The 26 S proteasome (10 μg/mL) was incubated without (panels a and d) or with Cu^{2+}/H_2O_2 (panels b and e, 100 μM $Cu^{2+}$and 0.5 mM H_2O_2; panels c and f, 100 μM $Cu^{2+}$and 1 mM H_2O_2) for 30 min and was treated with 1 mM biotin-LC-hydrazide for 1 h. The biotin-LC-hydrazide-labeled proteins were separated on two-dimensional gel electrophoresis (panels a−c) and then analyzed by Western blot probed with streptavidin−HRP (panels d−f). (B) Identification of a specific target of ROS in 26 S proteasome. The oxidized proteasome treated with Cu^{2+}/H_2O_2 (100 μM Cu^{2+} and 0.5 mM H_2O_2) for 30 min was labeled with biotin-LC-hydrazide-and separated on two-dimensional gel electrophoresis and analyzed by Western blot probed with streptavidin−HRP or Western blot using an anti-S6 ATPase polyclonal antibody. Left panel, SYPRO Ruby fluorescence staining; middle panel, Western blot probed with streptavidin−HRP; right panel, Western blot analysis using an anti-S6 ATPase polyclonal antibody.

oxidative modification of S6 ATPase may be functionally associated with the altered recognition and degradation of proteasomal substrates in the cells.

Selective Oxidation of S6 ATPase upon Metal-Catalyzed Oxidation of Purified 26S Proteasome. To evaluate the oxidative modification of proteasome by ROS in vitro, we incubated the purified 26 S proteasome with a metal-catalyzed ROS generating system (Cu^{2+}/H_2O_2) and analyzed the target subunit of protein carbonylation. As shown in Figure 5A, when subjected to the electrophoresis, the native (unoxidized) form of proteasome migrates as two protein bands, corresponding to 26 S and 20 S proteasomes, in the polyacrylamide gel electrophoresis. Cu^{2+} alone, at the maximum concentration used in the metal-catalyzed oxidation system (10 μM), did not exert any significant effect on both 20 S and 26 S proteasomes. Upon incubation with the metal-catalyzed ROS generating system (Cu^{2+}/H_2O_2), 26 S proteasome was converted to lower molecular weight protein species in a Cu^{2+} concentration-dependent manner, whereas the protein band corresponding to 20 S proteasome was virtually unchanged, suggesting that changes in 26 S proteasome might be due to the oxidative modification of 19 S regulatory subunit(s). Then, we examined generation of the protein-linked carbonyl groups in the oxidized 26 S proteasome. The purified 26 S proteasome was incubated with H_2O_2 in the presence of Cu^{2+}, labeled with biotin-LC-hydrazide, and analyzed by ELISA or separated on two-dimensional gel electrophoresis followed by Western blot analysis. As shown in Figure 5B, ELISA analysis showed that the reaction of 26 S proteasome with Cu^{2+}/H_2O_2 resulted in a significant increase in protein carbonyls. In addition, Western blot analysis clearly revealed that protein carbonyls were mainly generated on a 48-kDa protein (Figure 5C).

To identify the oxidized subunit in 26 S proteasome, native and oxidized 26 S proteasome with Cu^{2+}/H_2O_2 were labeled with the biotin-LC-hydrazide and separated on the two-dimensional gel electrophoresis and analyzed by Western blot probed with streptavidin−HRP. Consistent with the one-dimensional gel electrophoresis (Figure 5C), a 48-kDa protein

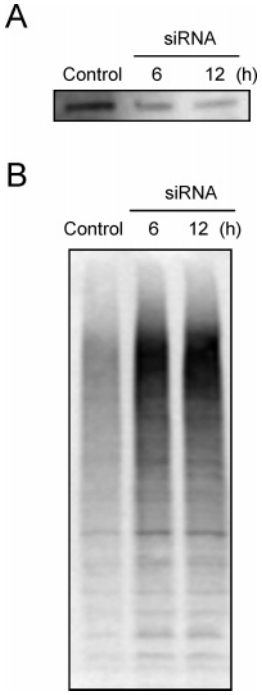

FIGURE 7: Down-regulation of S6 ATPase enhances accumulation of ubiquitinated proteins. (A) Immunoblot analysis of S6 ATPase in SH-SY5Y cells treated with specific siRNA of S6 ATPase. (B) Immunoblot analysis of ubiquitinated proteins in SH-SY5Y cells treated with specific siRNA of S6 ATPase.

was almost exclusively detected as the target of ROS generated during the metal-catalyzed oxidation reaction (Figure 6A). A proteomic analysis of this spot revealed that the proteasome subunit specifically oxidized was identical to S6 ATPase [using MASCOT, the provability-based MOWSE score was 154 for S6 ATPase ($p < 0.05$), with 19 peptide matches (error ±0.01%), which represents 26% sequence coverage (Supporting Information, Figure S2 and Table SII)]. The identity of S6 ATPase was further confirmed by Western blot analysis using an anti-S6 ATPase polyclonal antibody (Figure 6B). Thus, these in vitro studies have proved that S6 ATPase represents one of the most sensitive targets of ROS among the 26 S proteasome subunits.

Effect of RNAi of S6 ATPase on 26 S Proteasome Activity. Finally, to establish that S6 ATPase inhibition is associated with the impairment of proteasome function, we utilized RNAi to block expression of the proteasome subunit in SH-SY5Y cells. The cells were treated with siRNA corresponding to the S6 ATPase subunit (S6-siRNA), and the protein level of S6 ATPase was assessed by immunoblot analysis. As shown in Figure 7A, the protein level of S6 ATPase was significantly reduced by RNAi. To determine the effect of RNAi on proteasomal degradation, we blotted extracts of control and S6-siRNA-treated SH-SY5Y cells with an anti-ubiquitin antibody. As shown in Figure 7B, the treatment of cells with S6-siRNA resulted in the enhanced accumulation of ubiquitinated proteins. These data suggest that oxidative modification of this regulatory subunit of proteasome may be functionally associated with the altered recognition and degradation of proteasomal substrates in the cells.

DISCUSSION

In our previous study, as part of an effort to identify the endogenous inducer of intracellular oxidative stress and to elucidate the molecular mechanism underlying the oxidative stress-mediated cell degeneration, we examined the oxidized fatty acid metabolites for their ability to induce intracellular ROS production in SH-SY5Y cell in vitro and found that the J_2 series of the PGs represent the most potent inducers (*11*). On the basis of the observations that (*i*) 15d-PGJ_2 partially reduced intracellular glutathione levels, (*ii*) 15d-PGJ_2 treatment of the cells resulted in a significant decrease in the glutathione peroxidase activity, (*iii*) the *N*-acetylcysteine pretreatment significantly inhibited both ROS production and cytotoxicity by 15d-PGJ_2, and (*iv*) the intracellular ROS production was accompanied by the alteration of the cellular redox status and the production of lipid peroxidation-derived highly cytotoxic aldehydes, the intracellular redox status appeared to represent a critical parameter for the PG-induced ROS production and cytotoxicity. On the basis of these findings, we have hypothesized that intracellular oxidative stress constitutes a pivotal step in the pathway of cellular dysfunction induced by the electrophilic molecule.

In the present study, to further investigate the molecular mechanism underlying the oxidative stress-mediated cell degeneration, we analyzed protein carbonyl, the most widely studied marker of protein oxidation, using biotin-LC-hydrazide as the molecular probe. Consistent with our previous findings that 15d-PGJ_2 stimulates intracellular oxidative stress monitored by lipid peroxidation (*12*) and protein *S*-thiolation (*14*), 15d-PGJ_2 treatment resulted in the accumulation of protein carbonyls (Figure 1). Strikingly, the protein carbonylation specifically occurred on a 19 S regulatory subunit S6 ATPase (Figure 2), which was associated with (*i*) a dramatic increase in protein carbonyls within S6 ATPase, (*ii*) a significant decrease in the S6 ATPase activities, and (*iii*) a decreased ability of 26 S proteasome to degrade substrates (Figure 4). Moreover, H_2O_2 treatment of the cells also gave rise to oxidative modification of S6 ATPase (Figure 3). These findings suggest that this subunit may represent the oxidation-sensitive proteins in the cells.

It is also notable that in vitro oxidation of the purified 26 S proteasome with the Cu^{2+}/H_2O_2 oxidation system resulted in selective oxidation of S6 ATPase (Figures 5 and 6). Metal-catalyzed oxidation of proteins is a highly selective reaction that occurs primarily at protein sites with transition metal-binding capacity. Therefore, based on the observation that S6 ATPase was identified as the selective target of the Cu^{2+}/H_2O_2 oxidation system, it is hypothesized that metal (Cu^{2+}) binding would make the S6 ATPase protein a relatively easy target of the metal-catalyzed oxidation. Although the detailed mechanism for this preferential oxidation of S6 ATPase by Cu^{2+}/H_2O_2 remains unclear, Cu^{2+} bound to specific metal-binding sites on S6 ATPase may react with H_2O_2 to generate a ROS, which immediately oxidizes neighboring amino acid residues to generate carbonyl groups on S6 ATPase. It has been proposed that, upon reaction of Cu^{2+} with H_2O_2, the hydroxyl radical bound to Cu^{2+} (Cu^{2+}-OH•) is generated by the Fenton-type reaction of reduced copper (Cu^{+}) with H_2O_2 and that this bound oxidant then attacks adjacent amino acid residues. In the meantime, formation of the high valent oxocopper (III) species (Cu^{3+}═O), a possible hydroxylating species of copper oxygenases including tyrosinase and dopamine β-hydroxylase (*20*), has also been proposed. Neither Cu^{2+}-OH• nor Cu^{3+}═O has been detected experimentally; however, it is not unlikely that the protein carbonyl

formation within S6 ATPase is provoked by these types of copper-bound free radicals.

S6 ATPase subunit of the 19 S regulatory complex of the 26 S proteasome is one of six nonredundant ATPases, all belonging to the AAA (ATPases associated with diverse cellular activities) superfamily (*21*), and has been shown to interact with other 19 S regulatory subunit, such as S6′ ATPase and S7 ATPase (*22*−*25*). Among ATP-dependent proteases, these hexameric ATPase complexes are associated with substrate unfolding and translocation into an enclosed chamber where proteolysis occurs. Thus, the impairment of the regulatory complex may be functionally associated with the altered recognition and degradation of proteasomal substrates. Indeed, accompanied by a dramatic increase in protein carbonyls within the S6 ATPase subunit, 15d-PGJ_2 treatment exerted a significant decrease in the ATPase activities (Figure 4). Moreover, down-regulation of S6 ATPase by RNAi resulted in the enhanced accumulation of ubiquitinated proteins (Figure 7). On the other hand, the human S6 ATPase has been shown to form a complex with gankyrin (*26*−*28*). Gankyrin is the first protein described to bind both to the 26 S proteasome and to proteins in other complexes containing cyclin-dependent kinase(s) and p53 ubiquitinating activities, providing a mechanism for delivering cell cycle regulating machinery and ubiquitinated substrates to the proteasome for degradation. Indeed, 15d-PGJ_2 has been reported to induce accumulation and phosphorylation of p53, which is accompanied by a preferential redistribution of the p53 protein in the nuclei of the cells and by a time-dependent increase in p53 DNA binding activity (*12*). Thus, the oxidative impairment of S6 ATPase by 15d-PGJ_2 may result in the altered regulation of this oncoprotein.

Apart from intracellular oxidative stress induced by 15d-PGJ_2, there are also alternative explanations for the effects of this electrophile on proteasome dysfunction. For example, (*i*) 15d-PGJ_2 may cause dissociation of a proteasome activator, such as 19 S cap or PA28 regulator. (*ii*) 15d-PGJ_2 may induce phosphorylation or other events through lasting changes in the proteasome structure with inhibitory effects. (*iii*) As reported by Mullally et al. (*29*), 15d-PGJ_2 may inhibit the proteasome pathway via inhibition of the cellular ubiquitin isopeptidase activity. We have also demonstrated that 15d-PGJ_2 covalently binds to proteasome in the cells (*30*). Indeed, our preliminary experiments have shown that, upon in vitro incubation with 26 S proteasome, 15d-PGJ_2 binds to a number of proteasome subunits, including S6 ATPase (Ishii and Uchida, unpublished observatrion). Thus, 15d-PGJ_2 is likely to inhibit the proteasome pathway not only through selective oxidation of the proteasome subunit but also through a mechanism by which 15d-PGJ_2 directly interacts with proteasome.

In summary, proteomics identification of oxidized (carbonylated) proteins in SH-SY5Y cells exposed to 15d-PGJ_2 revealed that S6 ATPase represents the oxidation-sensitive subunit in proteasome. Accompanied by a dramatic increase in protein carbonyls within S6 ATPase, the electrophile-induced oxidative stress resulted in significant decrease in the ATPase activities and a decreased ability of the 26 S proteasome to degrade substrates. Moreover, selective oxidation of S6 ATPase was also observed upon in vitro oxidation of purified 26 S proteasome with a metal-catalyzed oxidation system. Our results provide support for the hypothesis that free radicals generated upon electrophile-induced oxidative stress mediate declines in proteasome function, thereby altering the balance between protein oxidation, ubiquitination, and degradation. Future studies must identify sites and forms of oxidative modification to the S6 ATPase subunit in order to fully characterize specific mechanisms by which the proteasome is inactivated.

ACKNOWLEDGMENT

We thank Dr. Toshihiko Osawa (Nagoya University) for his helpful advice.

SUPPORTING INFORMATION AVAILABLE

MALDI-TOF MS spectra corresponding to GST P1 and S6 ATPase and tables showing the peptides identified by MALDI-TOF MS from spot no. 2 and a 48-kDa oxidized proteasome subunit. This material is available free of charge via the Internet at http://pubs.acs.org.

REFERENCES

1. Halliwell, B., and Gutteridge, J. (1999) *Free Radicals in Biology and Medicine*, Oxford University Press, New York.
2. Sundaresan, M., Yu, Z.-X., Ferrans, V. J., Irani, K., and Finkel, T. (1995) Requirement for generation of H_2O_2 for platelet-derived growth factor signal transduction, *Science 270*, 296−299.
3. Stadtman, E. R. (1992) Protein oxidation and aging, *Science 257*, 1220−1224.
4. Stadtman, E. R., and Levine, R. L. (2000) Protein oxidation, *Ann. N.Y. Acad. Sci. 899*, 191−208.
5. Levine, R. L., Williams, J. A., Stadtman, E. R., and Schacter, E. (1994) Carbonyl assays for determination of oxidatively modified proteins, *Methods Enzymol. 233*, 346−357.
6. Oliver, C. N., Ahn, B. W., Moerman, E. J., Goldstein, S., and Stadtman, E. R. (1987) Age-related changes in oxidized proteins, *J. Biol. Chem. 262*, 5488−5491.
7. Smith, C. D., Carney, J. M., Starke-Reed, P. E., Oliver, C. N., Stadtman, E. R., Floyd, R. A., and Markesbery, W. R. (1991) Excess brain protein oxidation and enzyme dysfunction in normal aging and in Alzheimer disease, *Proc. Natl. Acad. Sci. U.S.A. 88*, 10540−10543.
8. Bowling, A. C., Schulz, J. B., Brown, R. H., Jr., and Beal, M. F. (1993) Superoxide dismutase activity, oxidative damage, and mitochondrial energy metabolism in familial and sporadic amyotrophic lateral sclerosis, *J. Neurochem. 61*, 2322−2325.
9. Gladstone, I. M., Jr., and Levine, R. L. (1994) Oxidation of proteins in neonatal lungs, *Pediatrics 93*, 764−768.
10. Berlett, B. S., and Stadtman, E. R. (1997) Protein oxidation in aging, disease, and oxidative stress, *J. Biol. Chem. 272*, 20313−20316.
11. Kondo, M., Oya-Ito, T., Kumagai, T., Osawa, T., and Uchida, K. (2001) Cyclopentenone prostaglandins as potential inducers of intracellular oxidative stress, *J. Biol. Chem. 276*, 12076−12083.
12. Kondo, M., Shibata, T., Kumagai, T., Osawa, T., Shibata, N., Kobayashi, M., Sasaki, S., Iwata, M., Noguchi, N., and Uchida, K. (2002) 15-Deoxy-$\Delta^{12,14}$-prostaglandin J_2: the endogenous electrophile that induces neuronal apoptosis, *Proc. Natl. Acad. Sci. U.S.A. 99*, 7367−7372.
13. Salmain, M., Fischer-Durand, N., Cavalier, L., Rudolf, B., Zakrzewski, J., and Jaouen, G. (2002) Transition metal−carbonyl labeling of biotin and avidin for use in solid-phase carbonyl metallo immunoassay (CMIA), *Bioconjugate Chem. 13*, 693−698.
14. Ishii, T., and Uchida, K. (2004) Induction of reversible cysteine-targeted protein oxidation by an endogenous electrophile 15-deoxy-$\Delta^{12,14}$-prostaglandin J_2, *Chem. Res. Toxicol. 17*, 1313−1322.
15. Baumeister, W., Walz, J., Zuhl, F., and Seemuller, E. (1998) The proteasome: paradigm of a self-compartmentalizing protease, *Cell 92*, 367−380.
16. Ciechanover, A. (1998) The ubiquitin-proteasome pathway: on protein death and cell life, *EMBO J. 17*, 7151−7160.

17. Glickman, M. H., and Ciechanover, A. (2002) The ubiquitin-proteasome proteolytic pathway: destruction for the sake of construction, *Physiol. Rev. 82*, 373−428.
18. Dubiel, W., Ferrell, K., and Rechsteiner, M. (1995) Subunits of the regulatory complex of the 26S protease, *Mol. Biol. Rep. 21*, 27−34.
19. Tanaka, K., and Tsurumi, C. (1997) The 26S proteasome: subunits and functions, *Mol. Biol. Rep. 24*, 3−11.
20. Stewart, L. C., and Klinman, J. P. (1987) Characterization of alternate reductant binding and electron transfer in the dopamine β-monooxygenase reaction, *Biochemistry 26*, 5302−5309.
21. Ogura, T., and Wilkinson, A. J. (2001) AAA^+ superfamily ATPases: common structure-diverse function, *Genes Cells 6*, 575−597.
22. Choi, H. S., Seol, W., and Moore, D. D. (1996) A component of the 26S proteasome binds on orphan member of the nuclear hormone receptor superfamily, *J. Steroid Biochem. Mol. Biol. 56*, 23−30.
23. Hartmann-Peterson, R., Tanaka, K., and Hendil, K. B. (2001) Quaternary structure of the ATPase complex of human 26S proteasome determined by chemical cross-linking, *Arch. Biochem. Biophys. 386*, 89−94.
24. Ohana, B., Moore, P. A., Ruben, S. M., Southgate, C. D., Green, M. R., and Rosen, C. A. (1993) The type 1 human immunodeficiency virus Tat binding protein is a transcriptional activator belonging to an additional family of evolutionarily conserved genes, *Proc. Natl. Acad. Sci. U.S.A. 90*, 138−142.
25. Uetz, P., Giot, L., Cagney, G., Mansfield, T. A., Judson, R. S., Knight, J. R., Lockshon, D., Narayan, V., Srinivasan, M., Pochart, P., Qureshi-Emili, A., Li, Y., Godwin, B., Conover, D., Kalbfleisch, T., Vijayadamodar, G., Yang, M., Johnston, M., Fields, S., and Rothberg, J. M. (2000) A comprehensive analysis of protein−protein interactions in *Saccharomyces cerevisiae*, *Nature 403*, 623−627.
26. Dawson, S., Apcher, S., Mee, M., Higashitsuji, H., Baker, R., Uhle, S., Dubiel, W., Fujita, J., and Mayer, R. J. (2002) Gankyrin is an ankyrin-repeat oncoprotein that interacts with CDK4 kinase and the S6 ATPase of the 26 S proteasome, *J. Biol. Chem. 277*, 10893−10902.
27. Krzywda, S., Brzozowski, A. M., Higashitsuji, H., Fujita, J., Welchman, R., Dawson, S., Mayer, R. J., and Wilkinson, A. J. (2004) The crystal structure of gankyrin, an oncoprotein found in complexes with cyclin-dependent kinase 4, a 19 S proteasomal ATPase regulator, and the tumor suppressors Rb and p53, *J. Biol. Chem. 279*, 1541−1545.
28. Fu, X. Y., Wang, H. Y., Tan, L., Liu, S. Q., Cao, H. F., and Wu, M. C. (2002) Overexpression of p28/gankyrin in human hepatocellular carcinoma and its clinical significance, *World J. Gastroenterol. 8*, 638−643.
29. Mullally, J.E., Moos, P. J., Edes, K., and Fitzpatrick, F. A. (2001) Cyclopentenone prostaglandins of the J series inhibit the ubiquitin isopeptidase activity of the proteasome pathway, *J. Biol. Chem. 276*, 30366−30373.
30. Shibata, T., Yamada, T., Kondo, M., Tanahashi, N., Tanaka, K., Nakamura, H., Masutani, H., Yodoi, J., and Uchida, K. (2003) An endogenous electrophile that modulates the regulatory mechanism of protein turnover: inhibitory effects of 15-deoxy-$\Delta^{12,14}$-prostaglandin J_2 on proteasome, *Biochemistry 42*, 13960−13968.

BI051336U